# Thermogradient Dimensional Stabilization of eddential Cross-Sections of the Carrying Structure of an Autonomous Object


**Yulia Savelieva, Michael Livshits, Igor Adeyanov, and Ivan Danilushkin**

**Abstract** The operating efficiency of autonomous objects of different purposes (underwater vehicles, spacecraft, etc.) substantially depends on the quality of the information received from heat-releasing apparatuses arranged on a carrying structure of the autonomous object. The thermal deformation of the carrying framework is caused by the irregularity of the temperature field due to a heat-releasing of devices, unsteady heat exchange with the ambient, and other reasons. In this case, the thermal deformation of the supporting framework, caused by the non-uniformity of the temperature field due to the heat dissipation of devices, unsteady heat transfer with the environment, and other reasons, is an important component of the complex distortion of information, especially optical measuring devices due to the displacement of the optical axis, focal length, etc., under the influence of a thermal gradient. Different systems of automatic thermal-stabilization are applied in order to decrease said distortions. The chapter is devoted to the mathematical modeling of thermal processes in the supporting framework during its automatic thermal gradient stabilization.

**Keywords** Autonomous object · Thermal-stabilization · Temperature distribution · Thermogradient stabilization system · Heat source

## 1 Introduction

Most devices arranged on a carrying structure of an autonomous object emits heat when operating, and it may cause thermal deformation, which, in turn, negatively affects the operation's efficiency of the information-measuring system comprising optical equipment [1–3]. The problem of stabilization of the average value of the temperature distribution as well as the reduction of its irregularity in order to exclude

Y. Savelieva (✉)
Branch of Samara State Technical University in Syzran, 45, Sovetskaya st, Syzran 446001, Russia
e-mail: Savelieva_yu_ol@mail.ru

M. Livshits · I. Adeyanov · I. Danilushkin
Samara State Technical University, 244, Molodogvardeyskaya st, Samara 443100, Russia
e-mail: usat@samgtu.ru



A. G. Kravets et al. (eds.), *Cyber-Physical Systems: Design and Application for Industry 4.0*, Studies in Systems, Decision and Control 342,
https://doi.org/10.1007/978-3-030-66081-9_2

thermogradient instability of the carrying framework shape is of current interest. The irregularity of the temperature distribution can be significantly reduced by arranging additional controlled heat-releasing elements (means of thermal gradient stabilization—hereinafter referred to as MTGS) and/or using a liquid cooling system. To analyze the operating mode of the heat-releasing devices and MTGS, to synthesize effective stabilization systems for the temperature distribution of the carrying framework, a mathematical model of its (framework's) temperature state is required.

## 2 Problem Statement

The carrying framework of the information-measuring system of the autonomous object is considered. The said framework has a shape of a rectangular prism (plate) and is subject to the influence of various thermal deformation loads. The plate (Fig. 1a) is cooled under the effect from the environment (the boundary condition of the third kind is BC-3) and is heated at the points of contact with the heat-releasing measuring devices: Pr1-Pr4, Pru1-Pru4, C1, h1, C2, h2, Pra, Prb, operating according to the cyclograms shown in Figs. 2, 3, 4, 5, 6 and 7 [4, 5] for one typical cycle with period $t_1 = 30{,}000$ s, and being controlled by MTGS: St1-St9, S1-S9. The basic initial data required for the calculations are presented in Tables 1 and 2.

The coordinates of the centers of the heat-releasing devices. Central MTGS on the plate's side $x = 0$: St1, St2, St3, St4, St5. Central MTGS on the plate's side $x = R_1$: S1, S2, S3, S4, S5. Diagonal MTGS on the plate's side $x = 0$ : St6, St7, St3, St8, St9. Diagonal MTGS on the plate's side $x = R_1$: S6, S7, S3, S8, S9. Heat-releasing

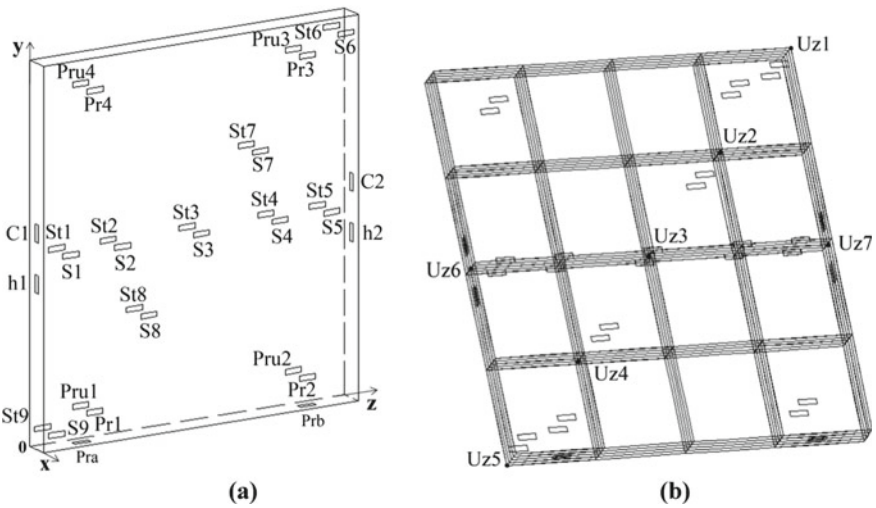


**Fig. 1** Carrying framework: **a** Arrangement of heat-releasing devices **b** Arrangement of control points

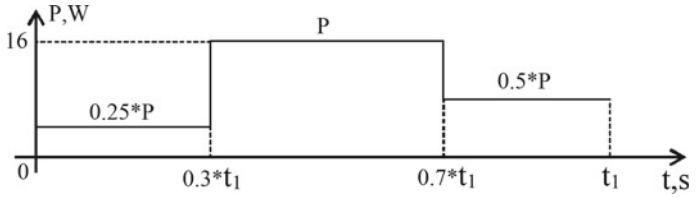


**Fig. 2** Cyclogram of changing in heat-releasing power of devices Pr1-Pr4

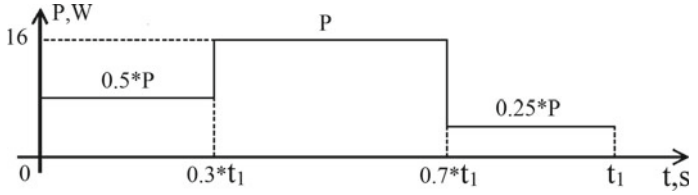


**Fig. 3** Cyclogram of changing in heat-releasing power of devices Pru1-Pru4

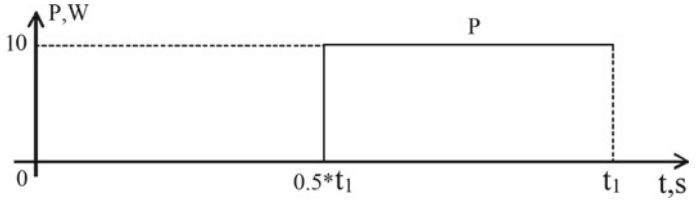


**Fig. 4** Cyclogram of changing in heat-releasing power of devices Pra-Prb

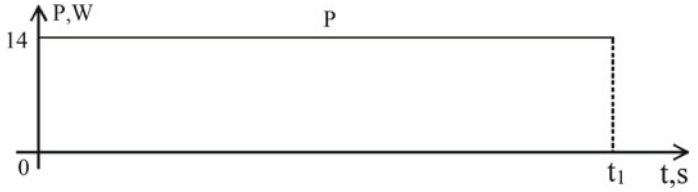


**Fig. 5** Cyclogram of changing in heat-releasing power of devices C1, C2

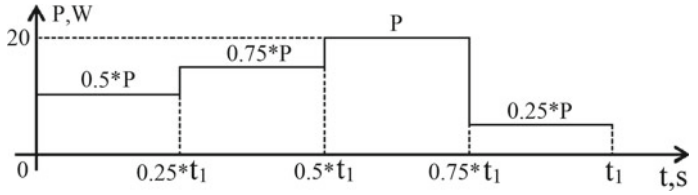


**Fig. 6** Cyclogram of changing in heat-releasing power of devices h1

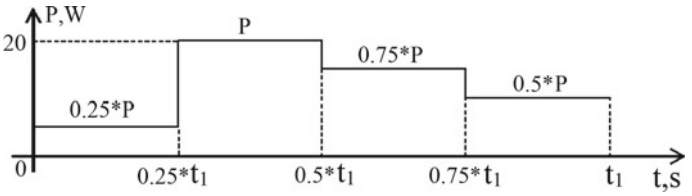


**Fig. 7** Cyclogram of changing in heat-releasing power of devices h2

**Table 1** Basic parameters

| | |
|---|---|
| *Geometry dimensions of the framework* | |
| $R_1$ dimensions of the plate along X axis, m | 0.15 |
| $R_2$ dimensions of the plate along Y axis, m | 2.15 |
| $R_3$ dimensions of the plate along Z axis, m | 1.97 |
| Thermophysical characteristics | |
| Specific heat capacity $c$, J/(kg·°C) | 1480 |
| Material density $\rho$, kg/m$^3$ | 1440 |
| Thermal conductivity λ, W/(m·°C) | 2.3 |
| Heat-transfer coefficient from body surface to environment $\alpha$, W/(m$^2$·°C) | 0.7488 |
| *Additional information* | |
| Environment temperature $T_{sred}$, °C | 20 |
| Initial temperature of the plate $T_{pl}^0$, °C | 40 |
| Dimensions of the seat for heat sources (S), m × m | 0.03, 0.1 |
| Biot number $Bi$ | 0.7 |

**Table 2** Nominal power of heat-releasing measuring devices

| Arrangement | Device | Power, W |
|---|---|---|
| Edge YZ,<br>x = 0, x = $R_1$ | Pr1–Pr4, Pru1–Pru4 | 16 |
| Edge XZ, y = 0 | Pra<br>Prb | 10<br>10 |
| Edge XY,<br>z = 0, z = $R_3$ | C1, C2<br>h1, h2 | 14<br>20 |

measuring devices on the plate's side $x = 0$: Pru1, Pru2, Pru3, Pru4. Heat-releasing measuring devices on the plate's side $x = R_1$: Pr1, Pr2, Pr3, Pr4. Heat-releasing measuring devices on the plate's side $y = 0$: Pra, Prb. Heat-releasing measuring devices on the plate's side $z = 0$: h1, C1. Heat-releasing measuring devices on the plate's side $z = R_3$: h2, C2.

The temperature field $\theta_{pl}(l_x, l_y, l_z, \phi)$ of the plate is described by the three-dimensional thermal conductivity equation [6–10]:

$$\frac{\partial\theta_{pl}(l_x,l_y,l_z,\phi)}{\partial\phi}=\frac{\partial^2\theta_{pl}(l_x,l_y,l_z,\phi)}{\partial l_x^2}+\frac{\partial^2\theta_{pl}(l_x,l_y,l_z,\phi)}{\partial l_y^2}+\frac{\partial^2\theta_{pl}(l_x,l_y,l_z,\phi)}{\partial l_z^2},$$
$$0<l_x<R_1\cdot R_2^{-1},\ 0<l_y<1,\ 0<l_z<R_3\cdot R_2^{-1},\phi\in(0;\infty), \quad (1)$$

by relative units: $y\cdot R_2^{-1}=l_y$, $x\cdot R_2^{-1}=l_x$, $z\cdot R_2^{-1}=l_z$, wherein $\phi=\frac{at}{R_2^2}$—Fourier number (« non-dimensional time »), $a=\frac{\lambda}{c\rho}$—thermal diffusivity, $\theta_{pl}(l_x,l_y,l_z,\phi)=(T_{pl}(x,y,z,t)-T^*)\cdot T^{*-1}$, $T^*=T_{sred}=const$—basic temperature, °C.

Initial condition:

$$\theta_{pl}(l_x,l_y,l_z,0)=(T_{pl}^0-T^*)\cdot T^{*-1}, \quad (2)$$

wherein $T_{pl}^0=const$—initial temperature of the plate, °C.

Boundary conditions:

$$\left.\frac{\partial\theta_{pl}(l_x,l_y,l_z,\phi)}{\partial l_x}\right|_{l_x=0}=Q_{pl}^{lx0}(l_y,l_z,\phi), \quad (3)$$

$$\left.\frac{\partial\theta_{pl}(l_x,l_y,l_z,\phi)}{\partial l_x}\right|_{l_x=R_1\cdot R_2^{-1}}=Q_{pl}^{lx1}(l_y,l_z,\phi), \quad (4)$$

$$\left.\frac{\partial\theta_{pl}(l_x,l_y,l_z,\phi)}{\partial l_y}\right|_{l_y=0}=Q_{pl}^{ly0}(l_x,l_z,\phi), \quad (5)$$

$$\left.\frac{\partial\theta_{pl}(l_x,l_y,l_z,\phi)}{\partial l_y}\right|_{l_y=1}=Q_{pl}^{ly1}(l_x,l_z,\phi), \quad (6)$$

$$\left.\frac{\partial\theta_{pl}(l_x,l_y,l_z,\phi)}{\partial l_z}\right|_{l_z=0}=Q_{pl}^{lz0}(l_x,l_y,\phi), \quad (7)$$

$$\left.\frac{\partial\theta_{pl}(l_x,l_y,l_z,\phi)}{\partial l_z}\right|_{l_z=R_3\cdot R_2^{-1}}=Q_{pl}^{lz1}(l_x,l_y,\phi). \quad (8)$$

Here $\theta_{pl}^{lx0}(l_y,l_z,\phi)$, $\theta_{pl}^{lx1}(l_y,l_z,\phi)$, $\theta_{pl}^{ly0}(l_x,l_z,\phi)$, $\theta_{pl}^{ly1}(l_x,l_z,\phi)$, $\theta_{pl}^{lz0}(l_x,l_y,\phi)$, $\theta_{pl}^{lz1}(l_x,l_y,\phi)$—summarized heat flow on the corresponding edges of the framework:

$$Q_{pl}^{lx0}(l_y,l_z,\phi)=q_p(\phi)-\sum_{i=1}^{N}q^i\cdot V_{l\times0}^i(l_y,l_z), \quad (9)$$

$$Q_{pl}^{lx1}(l_y, l_z, \phi) = -q_p(\phi) + \sum_{i=1}^{N} q_{l\times 1}^{i} \cdot V_{l\times 1}^{i}(l_y, l_z), \tag{10}$$

$$Q_{pl}^{ly0}(l_x, l_z, \phi) = q_p(\phi) - \sum_{i=1}^{M} q_{ly0}^{i} \cdot V_{ly0}^{i}(l_x, l_z), \tag{11}$$

$$Q_{pl}^{ly1}(l_x, l_z, \phi) = -q_p(\phi) + \sum_{i=1}^{M} q_{ly1}^{i} \cdot V_{ly1}^{i}(l_x, l_z), \tag{12}$$

$$Q_{pl}^{lz0}(l_x, l_y, \phi) = q_p(\phi) - \sum_{i=1}^{K} q_{lz0}^{i} \cdot V_{lz0}^{i}(l_x, l_y), \tag{13}$$

$$Q_{pl}^{lz1}(l_x, l_y, \phi) = -q_p(\phi) + \sum_{1=1}^{K} q_{lz1}^{i} \cdot V_{lz1}^{i}(l_x, l_y). \tag{14}$$

$q_p(\phi)$—flows of heat losses from the surface, which are assumed to be the same on all surfaces of the plate; $q_{lx0}^{i}$, $q_{lx1}^{i}$—flows from the heat sources arranged on the edges $l_x = 0$ and $l_x = R_1 \cdot R_2^{-1}$ accordingly, $q_{ly0}^{i}$, $q_{ly1}^{i}$—flows from the heat sources arranged on the edges $l_y = 0$ and $l_y = 1$ accordingly, $q_{lz0}^{i}$, $q_{lz1}^{i}$—flows from the heat sources arranged on the edges $l_z = 0$ and $l_z = R_3 \cdot R_2^{-1}$ accordingly, wherein the intensity of flows from the heat sources is defined as a ratio of heat emission power P of the corresponding device to its area S of contact with the plate surface $q^i = P \cdot S^{-1}$; $V_{lx0}^{i}(l_y, l_z)$, $V_{lx1}^{i}(l_y, l_z)$—functions determining the location of the devices on the edges $l_x = 0$ and $l_x = R_1 \cdot R_2^{-1}$ accordingly, $V_{ly0}^{i}(l_x, l_z)$, $V_{ly1}^{i}(l_x, l_z)$—functions determining the location of the devices on the edges $l_y = 0$ and $l_y = 1$ accordingly, $V_{lz0}^{i}(l_x, l_y)$, $V_{lz1}^{i}(l_x, l_y)$—functions determining the location of the devices on the edges $l_z = 0$ and $l_z = R_3 \cdot R_2^{-1}$ accordingly.

The temperature distribution in the plate is determined by solving auxiliary three-dimensional boundary value problem (1)–(8) according to the following algorithm:

1. Solving $\theta_{pl}(l_x, l_y, l_z, \phi)$ three-dimensional boundary value problem (1)–(8) is considered as the product of $\theta_{pl}(l_x, \phi)$, $\theta_{pl}(l_y, \phi)$ and $\theta_{pl}(l_z, \phi)$:

$$\theta_{pl}(l_x, l_y, l_z, \phi) = \theta_{pl}(l_x, \phi) \cdot \theta_{pl}(l_y, \phi) \cdot \theta_{pl}(l_z, \phi)$$

   solving the corresponding boundary value problems [11, 12] under condition $q_{lx}^{i} = 0$, $q_{ly}^{i} = 0$, $q_{lz}^{i} = 0$, influence thereof is reflected by the summation of said solving and corresponding solving of three-dimensional boundary value problem with the boundary condition of the second kind (BC-2).
2. The convective nature of the heat exchange of the plate with the environment (BC-3) is reflected by the equivalent model for BC-2.
   Figure 8 shows proposed in the paper [13] structural representation of one-dimensional third boundary value problem BC-3 for $\theta_{pl}^{0} = 0$ by transfer functions

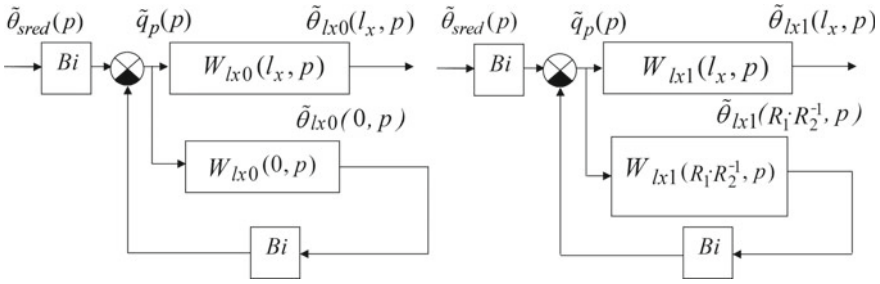


**Fig. 8** The framework of one-dimensional auxiliary boundary value problem $\theta_{pl}(l_x, \phi)$ by the Laplace transforms $\theta_{pl}(l_x, p)$

BC-2 $W_{lx0}(l_x, p)$, $W_{lx1}(l_x, p)$ accordingly for the one $l_x = 0$ and for the other $l_x = R_1 \cdot R_2^{-1}$ side of the plate.

Here $Bi = \alpha \cdot R_2 \cdot \lambda^{-1}$—Biot number. In the current example $\theta_{sred}(\phi) = (T_{sred}(t) - T^*) \cdot T^{*-1} = 0$.

The corresponding transforms $\theta_{pl}(l_y, p)$, $\theta_{pl}(l_z, p)$ of temperature distributions $\theta_{pl}(l_y, \phi)$, $\theta_{pl}(l_z, \phi)$ is determined in the same way.

3. The thermal effect from the heat-releasing devices and MTGS is determined independently, and then taken into account in the general problem (1)–(8) by summation of the corresponding components of the temperature field.

## 3 Interaction with the Environment

One-dimensional boundary value problems with BC-2 for $\theta_{pl}(l_x, \phi)$, $\theta_{pl}(l_y, \phi)$, $\theta_{pl}(l_z, \phi)$ used in the scheme (Fig. 8) are the following:

$$\begin{cases} \frac{\partial \theta_{pl}(l_x,\phi)}{\partial \phi} = \frac{\partial^2 \theta_{pl}(l_x,\phi)}{\partial l_x^2}, \ 0 < l_x < R_1 \cdot R_2^{-1}, \phi \in (0; \infty), \\ \theta_{pl}(l_x, 0) = \theta_{pl}^0, 0 \le l_x \le R_1 \cdot R_2^{-1}, \phi \in (0; \infty), \\ \left.\frac{\partial \theta_{pl}(l_x,\phi)}{\partial l_x}\right|_{lx=0} = q_p(\phi), \ \left.\frac{\partial \theta_{pl}(l_x,\phi)}{\partial l_x}\right|_{lx=R_1 \cdot R_2^{-1}} = -q_p(\phi). \end{cases} \tag{15}$$

$$\begin{cases} \frac{\partial \theta_{pl}(l_y,\phi)}{\partial \phi} = \frac{\partial^2 \theta_{pl}(l_y,\phi)}{\partial l_y^2}, \ 0 < l_y < 1, \phi \in (0; \infty), \\ \theta_{pl}(l_y, 0) = \theta_{pl}^0, 0 \le l_y \le 1, \phi \in (0; \infty), \\ \left.\frac{\partial \theta_{pl}(l_y,\phi)}{\partial l_y}\right|_{ly=0} = q_p(\phi), \ \left.\frac{\partial \theta_{pl}(l_y,\phi)}{\partial l_y}\right|_{ly=1} = -q_p(\phi). \end{cases} \tag{16}$$

$$\begin{cases} \frac{\partial \theta_{pl}(l_z,\phi)}{\partial \phi} = \frac{\partial^2 \theta_{pl}(l_z,\phi)}{\partial l_z^2}, 0 < l_z < R_3 \cdot R_2^{-1}, \phi \in (0; \infty), \\ \theta_{pl}(l_z, 0) = \theta_{pl}^0, 0 \le l_z \le R_3 \cdot R_2^{-1}, \phi \in (0; \infty), \\ \left.\frac{\partial \theta_{pl}(l_z,\phi)}{\partial l_z}\right|_{lz=0} = q_p(\phi), \ \left.\frac{\partial \theta_{pl}(l_z,\phi)}{\partial l_z}\right|_{lz=R_3 \cdot R_2^{-1}} = -q_p(\phi). \end{cases} \tag{17}$$

In order to solve said boundary value problems a finite integral transformations method is applied [13]:

$$\bar{\theta}_{pl}(\mu_n, \tau) = \int_0^{R_1 \cdot R_2^{-1}} \theta_{pl}(l_x, \phi)\varphi_n(\mu_n, l_x)r(l_x)dl_x, \tag{18}$$

$$\bar{\theta}_{pl}(\psi_m, \tau) = \int_0^{1} \theta_{pl}(l_y, \phi)\varphi_m(\psi_m, l_y)r(l_y)dl_y, \tag{19}$$

$$\bar{\theta}_{pl}(\gamma_k, \tau) = \int_0^{R_3 \cdot R_2^{-1}} \theta_{pl}(l_z, \phi)\varphi_k(\gamma_k, l_z)r(l_z)dl_z, \tag{20}$$

wherein $\bar{\theta}_{pl}(\mu_n, \psi_m, \gamma_k, \tau)$—transform of the original function; $r$—weight function (according to current problems $r = 1$); $\mu_n$, $\psi_m$, $\gamma_k$—proper numbers:

$$\mu_n = \frac{\pi n R_2}{R_1},\ n = 0, 1, 2, \ldots;\ \psi_m = \pi m,\ m = 0, 1, 2, \ldots;$$
$$\gamma_k = \frac{\pi k R_2}{R_3},\ k = 0, 1, 2, \ldots.$$

The normalized system of proper functions in one-dimensional problems has the form:

$$\varphi_n(\mu_n, l_x) = \frac{1}{E_n}\varphi_n^*(\mu_n, l_x) = \frac{1}{E_n}\cos(\pi n \frac{R_2 l_x}{R_1}),\ n = 0, 1, 2, \ldots,$$

$$\varphi_m(\psi_m, l_y) = \frac{1}{E_m}\varphi_m^*(\psi_m, l_y) = \frac{1}{E_m}\cos(\pi m l_y),\ m = 0, 1, 2, \ldots,$$

$$\varphi_k(\gamma_k, l_z) = \frac{1}{E_k}\varphi_k^*(\gamma_k, l_z) = \frac{1}{E_k}\cos(\pi k \frac{R_2 l_z}{R_3}),\ k = 0, 1, 2, \ldots,$$

Normalizing constants:

$$E_n = \sqrt{\int_0^{R_1 \cdot R_2^{-1}} \left[\varphi_n^*(\mu_n, l_x)\right]^2 r(l_x)dl_x} = \begin{cases} \sqrt{R_1 \cdot R_2^{-1}}, n = 0 \\ \sqrt{R_1 \cdot (2R_2)^{-1}}, n = 1, 2, 3 \ldots \end{cases},$$

$$E_m = \begin{cases} 1, m = 0 \\ \sqrt{0.5}, m = 1, 2, 3 \ldots \end{cases}, E_k = \begin{cases} \sqrt{R_3 \cdot R_2^{-1}}, k = 0 \\ \sqrt{R_3 \cdot (2R_2)^{-1}}, k = 1, 2, 3 \ldots \end{cases}.$$

Solving the boundary value problems (15)–(17) for BC-2 $\theta_{pl}(l_x, \phi)$, $\theta_{pl}(l_y, \phi)$, $\theta_{pl}(l_z, \phi)$ is the following:

$$\theta_{pl}(l_x, \phi) = \sum_{n=0}^{\infty} \varphi(\mu_n, l_x) \int_0^{\phi} R(\mu_n, \tau) G_n^*(\mu_n, \phi - \tau) d\tau + \sum_{n=0}^{\infty} \varphi(\mu_n, l_x) \int_0^{R_1 \cdot R_2^{-1}} \theta_{pl}^0 G_n^*(\mu_n, \phi) \varphi(\mu_n, \xi_{lx}) d\xi_{lx} \tag{21}$$

$$\theta_{pl}(l_y, \phi) = \sum_{m=0}^{\infty} \varphi(\psi_m, l_y) \int_0^{\phi} R(\psi_m, \tau) G_m^*(\psi_m, \phi - \tau) d\tau + \sum_{m=0}^{\infty} \varphi(\psi_m, l_y) \int_0^{1} \theta_{pl}^0 G_m^*(\psi_m, \phi) \varphi(\psi_m, \xi_{ly}) d\xi_{ly} \tag{22}$$

$$\theta_{pl}(l_z, \phi) = \sum_{k=0}^{\infty} \varphi(\gamma_k, l_z) \int_0^{\phi} R(\gamma_k, \tau) G_k^*(\gamma_k, \phi - \tau) d\tau + \sum_{k=0}^{\infty} \varphi(\gamma_k, l_z) \int_0^{R_3 \cdot R_2^{-1}} \theta_{pl}^0 G_k^*(\gamma_k, \phi) \varphi(\gamma_k, \xi_{lz}) d\xi_{lz} \tag{23}$$

wherein $R(\mu_n, \phi) = R_1(\mu_n, \phi) - R_0(\mu_n, \phi)$, $R(\psi_m, \phi) = R_1(\psi_m, \phi) - R_0(\psi_m, \phi)$, $R(\gamma_k, \phi) = R_1(\gamma_k, \phi) - R_0(\gamma_k, \phi)$—functions determined by the boundary conditions: $R_0(\mu_n, \phi) = q_p(\phi)\varphi_n(\mu_n, 0)$, $n = 0, 1, 2, 3 \ldots$,

$$R_0(\psi_m, \phi) = q_p(\phi)\varphi_m(\psi_m, 0),\ m = 0, 1, 2, 3 \ldots,$$

$$R_0(\gamma_k, \phi) = q_p(\phi)\varphi_k(\gamma_k, 0),\ k = 0, 1, 2, 3 \ldots,$$

$R_1(\mu_n, \phi) = -q_p(\phi)\varphi_n(\mu_n, R_1 \cdot R_2^{-1})$, $R_1(\psi_m, \phi) = -q_p(\phi)\varphi_m(\psi_m, 1)$, $R_1(\gamma_k, \phi) = -q_p(\phi)\varphi_k(\gamma_k, R_3 \cdot R_2^{-1})$. $G_n^*$, $G_m^*$, $G_k^*$—time components of the Green's function:

$$G_n^*(\mu_n, \phi) = e(-\mu_n^2 \phi) = e(-R_2^2 \pi^2 n^2 (R_1^2)^{-1} \phi),\ \ n = 0, 1, 2 \ldots, \tag{24}$$

$$G_m^*(\psi_m, \phi) = e(-\psi_m^2 \phi) = e(-\pi^2 m^2 \phi),\ \ m = 0, 1, 2 \ldots, \tag{25}$$

$$G_k^*(\gamma_k, \phi) = e(-\gamma_k^2 \phi) = e(-R_2^2 \pi^2 k^2 (R_3^2)^{-1} \phi),\ \ k = 0, 1, 2 \ldots, \tag{26}$$

Transfer functions (TF) used in the scheme (Fig. 8) for one-dimensional boundary value problem with BC-2 along $l_x, l_y, l_z$ and being the Laplace transforms of the corresponding Green's functions have the following form:

$$W_{lx}(l_x, p) = R_2 \cdot (R_1 p)^{-1} + 2R_2 \cdot R_1^{-1} \sum_{n=1}^{\infty} \cos(\pi n R_2 l_x \cdot R_1^{-1}) \times \cos(\pi n R_2 \xi_{lx} R_1^{-1}) R_1^2 (R_2^2 \pi^2 n^2)^{-1} (R_1^2 (R_2^2 \pi^2 n^2)^{-1} p + 1)^{-1} \quad (27)$$

$$W_{ly}(l_y, p) = p^{-1} + 2 \sum_{m=1}^{\infty} \cos(\pi m l_y) \cos(\pi m \xi_{ly}) \times (\pi^2 m^2)^{-1} ((\pi^2 m^2)^{-1} p + 1)^{-1} \quad (28)$$

$$W_{lz}(l_z, p) = R_2 \cdot (R_3 p)^{-1} + 2R_2 R_3^{-1} \sum_{k=1}^{\infty} \cos(\pi k R_2 l_z R_3^{-1}) \times \cos(\pi k R_2 \xi_{lz} R_3^{-1}) R_3^2 (R_2^2 \pi^2 k^2)^{-1} (R_3^2 (R_2^2 \pi^2 k^2)^{-1} p + 1)^{-1} \quad (29)$$

wherein $\xi$—corresponding spatial coordinate of the heat source arrangement, said heat source is considered as a control (disturbing) action. A design model for solving additional boundary value problems (15)–(17) under the condition $q_{lx}^i = 0$, $q_{ly}^i = 0$, $q_{lz}^i = 0$ may be created by dependencies (27)–(29) within using the scheme according to Fig. 8 in the MATLAB software.

## 4 Temperature Effect from the Heat Sources

The areas of contact of the heat sources with the plate surfaces $l_x = 0$, $l_x = R_1 \cdot R_2^{-1}$ along the corresponding coordinates are designated in Fig. 9: $A_{lx0}(0, A_{lx0}^y, A_{lx0}^z)$, $B_{lx0}(0, B_{lx0}^y, B_{lx0}^z)$, $C_{lx0}(0, C_{lx0}^y, C_{lx0}^z)$, $D_{lx0}(0, D_{lx0}^y, D_{lx0}^z)$; $A_{lx1}(R_1 \cdot R_2^{-1}, A_{lx1}^y, A_{lx1}^z)$, $B_{lx1}(R_1 \cdot R_2^{-1}, B_{lx1}^y, B_{lx1}^z)$, $C_{lx1}(R_1 \cdot R_2^{-1}, C_{lx1}^y, C_{lx1}^z)$, $D_{lx1}(R_1 \cdot R_2^{-1}, D_{lx1}^y, D_{lx1}^z)$.

The boundary value problem for the temperature component $\theta_{ist}(l_x, l_y, l_z, \phi)$ of the heat sources effect is as follows:

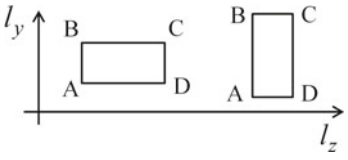


**Fig. 9** General designation of the heat sources coordinates when $l_x$ fixed

$$\frac{\partial\theta_{ist}(l_x,l_y,l_z,\phi)}{\partial\phi}=\frac{\partial^2\theta_{ist}(l_x,l_y,l_z,\phi)}{\partial l_x^2}+\frac{\partial^2\theta_{ist}(l_x,l_y,l_z,\phi)}{\partial l_y^2}+\frac{\partial^2\theta_{ist}(l_x,l_y,l_z,\phi)}{\partial l_z^2},0<l_x<\frac{R_1}{R_2},\ 0<l_y<1,\ 0<l_z<\frac{R_3}{R_2},\phi\in(0;\phi_k). \quad (30)$$

Initial conditions: $\theta_{ist}(l_x,l_y,l_z,0)=0$. Boundary conditions along axis $l_x$:

$$\left.\frac{\partial\theta_{ist}(l_x,l_y,l_z,\phi)}{\partial l_x}\right|_{lx=0}=-\sum_{i=0}^{\infty}q_{lx0}^{i}\left[1(l_y-A_{lx0}^{y})-1(l_y-B_{lx0}^{y})\right]\cdot\left[1(l_z-A_{lx0}^{z})-1(l_z-D_{lx0}^{z})\right], \quad (31)$$

$$\left.\frac{\partial\theta_{ist}(l_x,l_y,l_z,\phi)}{\partial l_x}\right|_{lx=R_1\cdot R_2^{-1}}=\sum_{i=0}^{\infty}q_{lx1}^{i}\left[1(l_y-A_{lx1}^{y})-1(l_y-B_{lx1}^{y})\right]\cdot\left[1(l_z-A_{lx1}^{z})-1(l_z-D_{lx1}^{z})\right], \quad (32)$$

Boundary conditions along with the coordinates $l_y$ and $l_z$—formalized similarly. The components of the temperature distribution in the plate under the heat sources effect is determined by the corresponding convolution with the Green's function $G_{ist}(l_x,\xi_{lx},l_y,\xi_{ly},l_z,\xi_{lz},\phi-\tau)$ [14]:

$$\theta_{ist}(l_x,l_y,l_z,\phi)=\theta_{ist}^{lx}(l_x,l_y,l_z,\phi)+\theta_{ist}^{ly}(l_x,l_y,l_z,\phi)+\theta_{ist}^{lz}(l_x,l_y,l_z,\phi), \quad (33)$$

$$\theta_{ist}(l_x,l_y,l_z,\phi)=$$

$$-\sum_{l_x=0}\int_{\phi_1}^{\phi_2}\int_{A_{lx0}^{z}}^{D_{lx0}^{z}}\int_{A_{lx0}^{y}}^{B_{lx0}^{y}}q_{lx0}^{i}G_{ist}(l_x,\xi_{lx},l_y,\xi_{ly},l_z,\xi_{lz},\phi-\tau)d\xi_{ly}d\xi_{lz}d\tau$$

$$+\sum_{l_x=R_1\cdot R_2^{-1}}\int_{\phi_3}^{\phi_4}\int_{A_{lx1}^{z}}^{D_{lx1}^{z}}\int_{A_{lx1}^{y}}^{B_{lx1}^{y}}q_{lx1}^{i}G_{ist}(l_x,\xi_{lx},l_y,\xi_{ly},l_z,\xi_{lz},\phi-\tau)d\xi_{ly}d\xi_{lz}d\tau$$

$$-\sum_{l_y=0}\int_{\phi_1}^{\phi_2}\int_{A_{ly0}^{x}}^{D_{ly0}^{x}}\int_{A_{ly0}^{z}}^{B_{ly0}^{z}}q_{ly0}^{i}G_{ist}(l_x,\xi_{lx},l_y,\xi_{ly},l_z,\xi_{lz},\phi-\tau)d\xi_{lz}d\xi_{lx}d\tau$$

$$+\sum_{l_y=1}\int_{\phi_3}^{\phi_4}\int_{A_{ly1}^{x}}^{D_{ly1}^{x}}\int_{A_{ly1}^{z}}^{B_{ly1}^{z}}q_{ly1}^{i}G_{ist}(l_x,\xi_{lx},l_y,\xi_{ly},l_z,\xi_{lz},\phi-\tau)d\xi_{lz}d\xi_{lx}d\tau$$

$$-\sum_{l_z=0}\int_{\phi_1}^{\phi_2}\int_{A_{lz0}^{x}}^{D_{lz0}^{x}}\int_{A_{lz0}^{y}}^{B_{lz0}^{y}}q_{lz0}^{i}G_{ist}(l_x,\xi_{lx},l_y,\xi_{ly},l_z,\xi_{lz},\phi-\tau)d\xi_{ly}d\xi_{lx}d\tau$$

$$+\sum_{l_z=R_3\cdot R_2^{-1}}\int_{\phi_3}^{\phi_4}\int_{A_{lz1}^x}^{D_{lz1}^x}\int_{A_{lz1}^y}^{B_{lz1}^y} q_{lz1}^i G_{ist}(l_x,\xi_{lx},l_y,\xi_{ly},l_z,\xi_{lz},\phi-\tau)d\xi_{ly}d\xi_{lx}d\tau. \tag{34}$$

wherein

$$\begin{aligned} G_{ist}(l_x,\xi_{lx},l_y,\xi_{ly},l_z,\xi_{lz},\phi-\tau) = &\sum_{n=0}^{\infty} G_n^*(\mu_n,\phi-\tau)\varphi_n(\mu_n,l_x) \\ &\times \varphi_n(\mu_n,\xi_{lx})r(\xi_{lx})\cdot\sum_{m=0}^{\infty} G_m^*(\psi_m,\phi-\tau)\varphi_m(\psi_m,l_y) \\ &\times \varphi_m(\psi_m,\xi_{ly})r(\xi_{ly})\sum_{k=0}^{\infty} G_k^*(\gamma_k,\phi-\tau)\varphi_k(\gamma_k,l_z) \\ &\times \varphi_k(\gamma_k,\xi_{lz})r(\xi_{lz}). \end{aligned}$$

## 5 Result of Modeling

The mathematical model created in the MATLAB software on the basis of the obtained relations [15, 16] allows us to carry out the approximate synthesis of the controller, analysis of the corresponding control system stability and etc. A finite—element numerical modeling in the ANSYS software [17–19] is applied to problem solving more precisely.

We consider here the task of stabilizing the temperature in the critical cross-section of the carrying framework of the autonomous object (Fig. 1b) along the line from Uz1 to Uz5 by controlling the diagonal MTGS St6, St7, St3, St8, St9 on the one side of the prism and S6, S7, S3, S8, S9 on the other side thereof. The results of modeling the reaction of the temperature distribution in the carrying framework to the effect of the heat sources during t = 30,000 s in the ANSYS software are reflected in Fig. 10.

Figure 10b shows the temperature fields of the prism under the effect of diagonal MTGS St6, S6, St9, S9 with the power of 8 W.

The temperature graphs of the corresponding cross-section line are presented in Fig. 11, wherein the vertical axis $T_{pl}$, °C represents temperature values, and the horizontal axis D, m represents a diagonal cross-section from Uz1 to Uz5.

The results of the operation of the automatic temperature stabilization system in the critical node Uz1 being critical for providing the dimensional stabilization along the line of cross-section from Uz1 to Uz5 are subject to consideration. The closest heat sources influence Uz1 in a most substantial way: from the measuring devices in nodes Pr3, Pru3 being controlled by MTGS St6, S6, as well as the convective heat exchange with the environment.

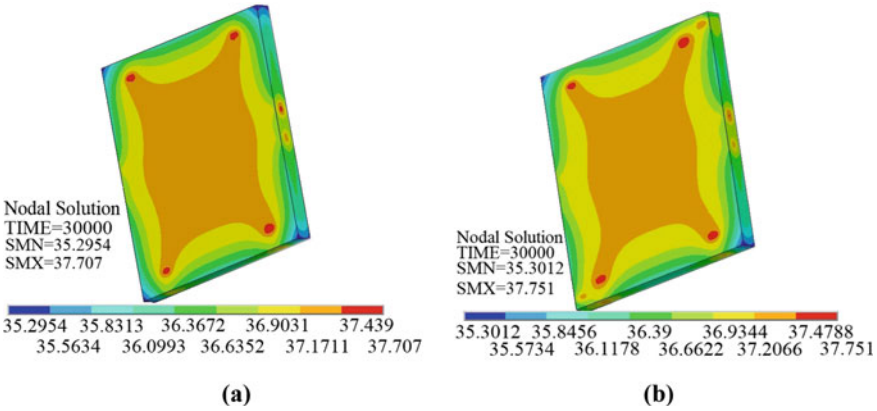


**Fig. 10** Finite-element modeling of the carrying framework temperature in the Ansys software (t = 30,000): **a** Without MTGS effect **b** When diagonal MTGS effect, wherein MTGS arranged along the line from Uz1 to Uz5

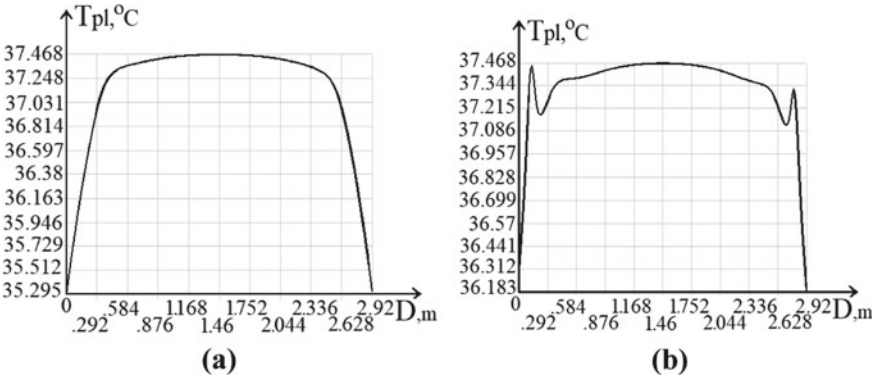


**Fig. 11** Graphs of temperature distribution for t = 30,000 s: **a** Along diagonal cross section from Uz1 to Uz5 without MTGS **b** Along diagonal cross section from Uz1 to Uz5 when MTGS effect

The algorithm of control of MTGS St6 and S6 effecting on the point of control Uz1 is implemented by the proportional—integral (PI) law of control (Figs. 12, 13).

There is an automatically formed the changing in the power of MTGS St6 and S6 in deviation from the average value of the MTGS power at the PI-controller output.

## 6 Conclusions

There have been presented an argument for the problem of automatic stabilization of temperature distribution in the carrying framework of the autonomous object as

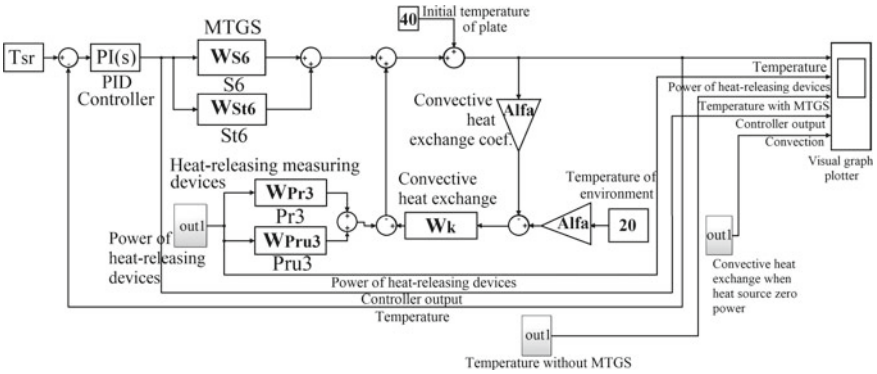


**Fig. 12** Scheme of modeling a temperature control system of the critical node of the carrying framework in the MATLAB software: Tsr—the predetermined temperature in the node Uz1, Alfa—the unit of determination of the heat exchange coefficient, α; WS6, WSt6, WPr3,WPru3, Wk—transfer functions determining the temperature in the node Uz1 when MTSG S6, St6, measuring devices Pr3, Pru3 and convective heat exchange effect, PID Controller—unit of modelling PI-controller (without derivative term)

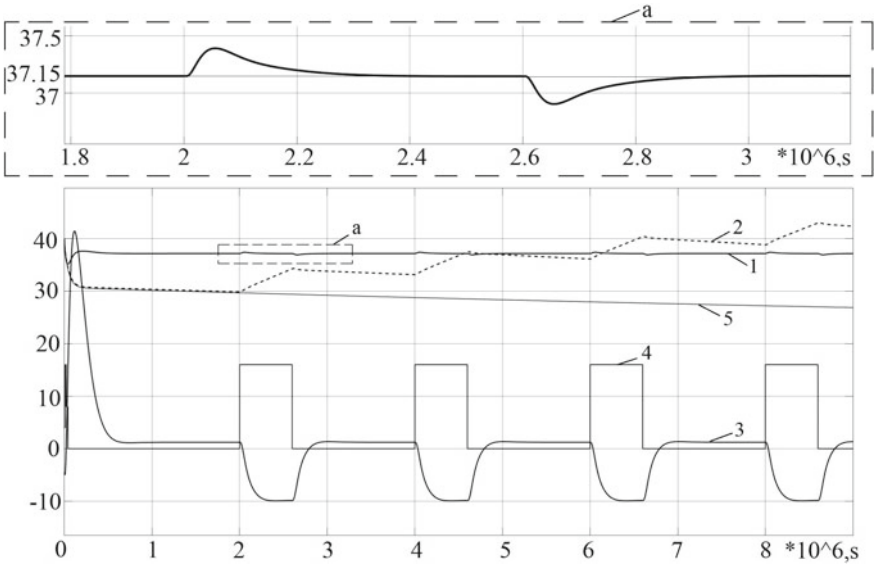


**Fig. 13** Result of modeling the automatic temperature stabilization system in the node in the MATLAB software: 1 Temperature in the node Uz1 under the automatic control, °C; 2 Temperature in the node Uz1 without control, °C; 3 Power of MTGS generated at the PI-controller output (control for MTGS), W; 4 Cyclogram of changing in heat-releasing power of the measuring devices, W; 5 Convectional heat losses, °C; a Portion of temperature distribution under the automatic control, °C

the effective means for decreasing the temperature component in the error of the information-measuring system arranged on the said framework.

There has been provided a method of mathematical modeling of the temperature distribution in the carrying frameworks of autonomous objects, said method comprises approximate mathematical modeling in the MATLAB software and more precise modeling in the ANSYS software.

By analytical structural-parametric identification, there have been obtained the transfer functions of the temperature distribution in the carrying framework for implementation in an approximate mathematical model in MATLAB software and controller synthesis.

Modeling of the automatic temperature stabilization system in the node of the critical cross-section of the supporting framework has confirmed its high efficiency.

**Acknowledgements** The present research has been carried out due to support of the Russian Foundation for Basic Research (project No. 20-08-00240)

## References

1. Livshits, M.Y., Derevyanov, M.Y., Kopytin, S.A.: Distributed optimal control of technological thermophysics objects. In Proceedings of the 4th All-Russian Multiconference on Management Problems, vol. 2, pp. 99–102. Taganrog, TTI YUFU (2011)
2. Livshits, M.Y., Derevyanov, M.Y., Davydov, A.N., Kopytin, S.A.: Stabilization of temperature field of autonomous objects carrying frameworks. In: Proceedings of the 9th All-Russian Scientific Conference with International Participation. Mathematical Modeling and Boundary Value Problems, No. 3, pp. 47–52. Samara (2013)
3. Livshits, M.Y., Borodulin, B.B., Nenashev, A.V., Savelieva, Yu.O.: Distributed control of temperature regimes of autonomous objects structural elements. Management and modeling issues in complex systems. In: Proceedings of the XXI International Conference, vol.1, pp. 349–352. Samara, OOO Ofort (2019)
4. Livshits, M.Y., Borodulin, B.B.: Comparative analysis of optimal temperature distributions in the responsible sections of load bearing structures. International youth scientific conference on heat and mass transfer in the thermal control system of technical and technological energy devices, HMTTSC 2017. MATEC WEB OF CONFERENCES. Tomsk, EDP Sciences (2017)
5. Livshits, M.Y., Borodulin, B.B.: Optimization of temperature distributions in critical sections of carrying structures. Proceedings of the Seventh Russian National Conference on Heat Exchange, vol. 3, pp. 148–151 Moscow, Publishing House MEI (2018)
6. Butkovskiy, A.G.: Characteristics of systems with distributed parameters: reference guide, Moscow, The main edition of the physical and mathematical literature of the publishing house Nauka, 224 p. (1979)
7. Savelieva, Yu.O.: The question of realization of math modeling of systems with distributed parameters. Sovremennye nauchnye issledovaniya i razrabotki. Moscow, Science CenterOlimp, No. 9 (26), pp. 350–352 (2018)
8. Livshits, M.Y.: Quasi-optimal space-time distributed control of heat and mass transfer processes. XIII All-Russian governance meeting. Moscow, VSPU-(2019)
9. Livshits, M.Y.: System optimization of processes of heat and mass transfer of process thermal physics. Mathematical methods in technique and technology MMTT-29. In: Proceedings of the XXIX International Conference, pp. 104–114. Saratov, Yuri Gagarin State Technical University of Saratov (2016)

10. Kartashov, E.M.: Analytical methods in the thermal conductivity theory of solids: study guide, revised edition, No. 3, 550 p. Moscow, Higher school (2001)
11. Lykov, A.V.: The thermal conductivity theory: manual for thermal engineering specialties of universities, 600 p. Higher school, Moscow (1967). (In Russian)
12. Rapoport, E.Y.: Software controllability of linear multidimensional systems with distributed parameters. In: Proceedings of the Russian Academy of Sciences. Management system theory, Moscow, Russian Academy of Sciences, No 2, 22. (2015) (In Russian)
13. Rapoport, E.Y.: Structural modeling of objects and control systems with distributed parameters: study guide, 299 p. Moscow, Higher School (2003)
14. Polyanin, A.D.: Manual of linear equations of mathematical physics, 576 p. FIZMATLIT, Moscow (2001)
15. MATLAB: Introduction into modern optimization methods of control systems. https://www.mathworks.com/matlabcentral/fileexchange/53032-interactive-link-between-matlab-and-ansys Accessed 15 Apr 2020
16. MathWorks: Nick.Interactive link between MATLAB and ANSYS https://www.mathworks.com/matlabcentral/fileexchange/53032-interactive-link-between-matlab-and-ansys Accessed 15 Apr 2020
17. Kaplun, A.B., Morozov, E.M., Olfereva, M.A.: ANSYS for engineers: practitioner guide, 272 p. Editorial URSS, Moscow (2003)
18. Basov, K.A.: ANSYS: user reference, 640 p. DMK Press, Moscow (2005)
19. ANSYS Users FORUM: Modeling heat exchange processes by using the ANSYS finite element analysis software/ Guidance material. https://cae-club.ru/sites/default/files/users/files/13/metodika_dlya_zadach_teploobmena_v_ansys_mechanical_apdl.pdf Accessed 9 Jan 2020